

WIND TUNNEL PRESSURE MEASUREMENT STUDIES ON A TALL BUILDING WITH ELLIPTIC CROSS-SECTION: EFFECT OF ANGLE OF WIND INCIDENCE

S A Afreen¹, A Abraham^{*2}, S Selvi Rajan³, Nagesh R Iyer⁴ and Sanya Maria Gomez⁵

¹P.G.Student, Department of Civil Engineering, SCMS School of Engineering and Technology, Karukutty, Kerala

^{*2}Corresponding Author, Senior Scientist, Wind Engg. Lab., CSIR-SERC, Taramani, Chennai, E-mail:

abraham@serc.res.in

³Chief Scientist, Wind Engg. Lab., CSIR-SERC, Taramani, Chennai

⁴Former Director, CSIR-SERC, Taramani, Chennai

⁵Assistant Professor, Department of Civil Engineering, SCMS School of Engineering and Technology, Karukutty, Kerala

Synopsis

Wind tunnel pressure measurement studies were carried out on a rigid model (geometric scale 1:300) of a tall elliptic building having minor axis of 100mm (b), major axis of 200mm (d) and height (h) of 700mm, under simulated open terrain in a Boundary Layer Wind Tunnel (BLWT) facility available at CSIR-SERC, Chennai. The measurement of pressures were made using 8 pressure sensors for 12 different angles of wind incidence, ' θ ' ranging between 0° (wind normal to minor axis) and 90° (wind normal to major axis). Based on the analysis, mean pressure coefficients, mean drag/lift force and torsion coefficients were obtained corresponding to reference pressures at the respective measurement levels. It is observed that the evaluated values of mean drag force coefficients increased with change in angles of wind incidence from 0° to 90°. The evaluated values of mean lift force coefficients increased with change in angles of wind incidence from 0° up to 40° and beyond which it decreased. The evaluated values of mean drag force coefficients were compared with the values reported in Codes of Practice viz. IS: 875 (Part 3) and AS-NZS 1170.2. The evaluated values were found to be comparable with the values reported in IS: 875 for $\theta = 90^\circ$ and in AS-NZS for $\theta = 0^\circ$.

Keywords: Boundary Layer Wind Tunnel, Tall Elliptic Building, Angles of Wind Incidence, Mean Pressure Coefficients, Mean Drag/Lift Force Coefficients, Correlation Coefficients

-----***-----

INTRODUCTION

Demand for tall buildings is rapidly increasing worldwide including in India due to their significant economic benefits in dense urban land use. Wind loads are one of the most important loads that influence the design of tall buildings. Using wind tunnel, different techniques are being adopted for quantification of wind loads and its associated dynamic response on tall buildings. One such technique is measuring the wind induced pressures on tall building model using pressure sensors, and importance of the pressure measurement technique is felt by the many researchers worldwide even today. But the information on force coefficients using pressure measurement on 3D tall building with elliptic cross-section under boundary layer flow is very scanty. Galloping instability characteristics on 2D bluff bodies with elliptic cross-section using pressure measurement/six component base balance techniques for angles of wind incidence from 0° to 90° were studied through wind tunnel testing by Alonso et al (2010). The effect of plan ratio, angle of wind incidence on mean and unsteady pressure coefficients, Strouhal number and wake geometry on 2D bluff bodies with elliptic cross-section

using pressure measurement technique were studied through wind tunnel testing by Wiland (1968) and Dikshit (1970). Identification of boundary layer detachments, recirculations, vortex shedding phenomenon and other flow structures on elliptic cross-section having different plan ratios using flow visualisation technique were studied through vertical hydrodynamic tunnel testing by Fonseca et al (2013). The effect of building shape (square, circular, triangular, rectangular and elliptical shapes) on the wind-induced response of a structure using high frequency force balance through a comprehensive investigation of wind tunnel studies performed at Rowan Williams Davies and Irwin, Inc. (RWDI) was reported by Merrick and Bitsuamlak (2009). The characteristics of aerodynamic forces acting on an elliptic cylinder with an angle of attack subjected to short-rise-time gusts using a specially-equipped gust wind tunnel were investigated by Takeuchi et al (2009). Codes of Practice viz. IS: 875 (Part 3) and AS-NZS 1170.2 specify the force coefficients for building with elliptic cross-section for two angles of wind incidence and for a given plan ratio. The aim of the present study is to investigate the external aerodynamic pressure distribution around a tall elliptic building model with plan dimensions of 10 cm x 20 cm and

with height of 70 cm and mean aerodynamic force coefficients for the simulation under considered for different angles of wind incidence. This paper presents results of variation on mean pressure coefficients at 8 different levels for typical angles of wind incidence viz. 0° (wind normal to minor axis) and 90° (wind normal to major axis), mean drag/lift force coefficients (in the direction and perpendicular to the direction of wind) and mean torsion coefficients (about vertical direction) at typical level (Level 4 corresponding to 35 cm, mid-height of the model) obtained through measurements of pressures using pressure sensors under simulated open terrain condition in BLWT facility available at CSIR-SERC, Chennai.

WIND TUNNEL INVESTIGATIONS ON TALL BUILDING MODEL

Details of the Model and Instrumentation

For the present study, a rigid model (geometric scale 1:300) with light weight material of acrylic/PVC sheet was used for wind tunnel investigations. The dimensions of the model are of 100 mm (b) x 200 mm (d), in plan, and height (h) of 700 mm. Elliptic shape stiffeners (guide plates) having minor axis of 98 mm and major axis of 198 mm of 10 numbers with a thickness of 6 mm are used as skeleton. These plates are placed at a spacing of 70 mm and are reinforced using a steel rod to maintain the geometry along the height, while wrapping the PVC sheet around the skeleton. Pressure ports were drilled to facilitate the pressure tubing system. The external surface of the model was instrumented with point pressure ports in azimuth direction at selected levels along the height. The pressure tubing system consisted of a special PVC tube having an internal diameter of 1.2 mm along with a restrictor and connecting between pressure port and pressure scanner. The model was instrumented with a total number of 224 pressure ports at 8 different levels having 28 pressure ports at each level with a spacing of 1.75 cm between consecutive ports. A total number of 8 Electronic pressure Scanners (ESP) scanners with 32 channels of each were employed. The levels at which the instrumentation was made and the corresponding z/h ratio are as follows: Level 1: z/h = 0.1; Level 2: z/h = 0.2; Level 3: z/h = 0.3; Level 4: z/h = 0.5; Level 5: z/h = 0.7; Level 6: z/h = 0.8; Level 7: z/h = 0.9 and Level 8: z/h = 0.95, where, 'h' is height of the model and 'z' is the height of instrumentation level, from base of the model. The schematic diagram of the pressure measurement system with pressure port details is shown in Figure 1.

Simulation of Wind Characteristics

The tall building is assumed to be located in open terrain category 2. Accordingly, profile of mean velocity, profile of turbulence intensity and turbulence spectrum of fluctuating wind corresponding to open terrain with a length scale of 1:300 were simulated in the wind tunnel by using a trip board followed by boards of wooden roughness elements, as vortex generators. The results on the above mentioned simulated wind characteristics are shown in Figure 2. The power law coefficient, ' α ' of the mean velocity and

turbulence intensity at roof of the model are found to be 0.14 and 10 %, respectively.

Wind Tunnel Investigations

Pressure measurements on tall building model with elliptic cross-section were carried out using BLWT available at CSIR-SERC, which is an open circuit and blower type wind tunnel. The total length of BLWT is 50 m, having a long test section of 18 m and with cross-sectional dimension of 2.5 m (Width) x 1.8 m (Height). Pressure measurements were made on the model for 12 different angles of wind incidence viz. 0° (wind normal to minor axis), 10° , 15° , 20° , 30° , 40° , 45° , 50° , 60° , 70° , 75° , 80° , 90° (wind normal to major axis) and for a mean wind velocity of 11 m/s, measured at the level of roof of building. Data were acquired with sampling rate of 700 samples per second per channel and for sampling duration of 15 sec. The surface pressure measurements were carried out using a high-speed 32-bit online Data Acquisition (DAQ) system. For each of the angle of wind incidence, 3 sets of data were acquired for reliable evaluation of mean pressure/force coefficients. Typical view of the model tested for $\theta = 0^\circ$ under simulated open terrain condition is shown in Figure 3.

DATA ANALYSIS

Evaluation of Pressure Coefficients

The instantaneous pressure coefficients $C_{p,i}(t)$ at the *i*th Level in time 't' can be defined as,

$$C_{p,i}(t) = p_i(t)/p_{ref} \quad (1)$$

where, p_{ref} = Reference pressure = $1/2 \rho \bar{U}_{ref}^2$; \bar{U}_{ref} = mean wind velocity at reference height z_i ($z_1 = 0.1h$: Level 1, $z_2 = 0.2h$: Level 2, $z_3 = 0.3h$: Level 3, $z_4 = 0.5h$: Level 4, $z_5 = 0.7h$: Level 5, $z_6 = 0.8h$: Level 6, $z_7 = 0.9h$: Level 7 and $z_8 = 0.95h$: Level 8); h = height of the model and ρ = mass density of air taken as 1.2 kg/m³.

The mean pressure coefficients $\bar{C}_{p,i}$ at the *i*th Level in time 't' can be defined as,

$$\bar{C}_{p,i} = 1/T \int_0^T C_{p,i}(t) dt \quad (2)$$

where, T = averaging period.

Evaluation of Correlation Coefficients of the Fluctuating Pressures

The correlation coefficient CC_{ij} of fluctuating pressures in time domain is defined as follows:

$$CC_{ij} = \sigma_{ij} / (\sigma_i \sigma_j) \quad (6)$$

where, σ_{ij} is covariance of wind pressures between ports *i* and *j*, σ_i and σ_j are the standard deviation values of wind pressures at ports *i* and *j*, respectively. In order to investigate the correlations, all the ports which are aligned vertically (along the height) and horizontally (around the bluff body at a typical level) with respect to windward port at stagnation point for $\theta = 0^\circ$ and 90° .

Evaluation of Mean Drag/Lift Force and Torsion

Coefficients

With reference to a fixed set of body axes (X and Y), orientations for forces F_x , F_y , and Torsion (T), along with drag and lift directions corresponding to angle of wind incidence ' θ ' are defined in Figure 1. The forces F_x and F_y per unit height along the body fixed axes X and Y, respectively, are computed by integrating the circumferentially measured pressures along with respective reference widths. By resolving F_x and F_y in the direction of wind and perpendicular to the direction of wind, the drag force F_d and the lift force F_l are evaluated. The mean drag and lift force coefficients are obtained at each level, using the following expressions:

$$\bar{C}_d = \frac{\bar{F}_d}{W_{ref} P_{ref}} \quad (3)$$

$$\bar{C}_l = \frac{\bar{F}_l}{W_{ref} P_{ref}} \quad (4)$$

where, \bar{F}_d , \bar{F}_l = Mean drag and lift forces, respectively; \bar{C}_d , \bar{C}_l = Mean drag and lift force coefficients, respectively; W_{ref} = Reference width = 'b' for \bar{C}_d , 'd' for \bar{C}_l ; P_{ref} = Reference pressure at measurement levels, as mentioned in Equation (1).

Torsion (T) for all angles of wind incidence with respect to the origin was evaluated using the measured pressures along with lever arms at each level. The mean torsion coefficients for each level were evaluated using the following expression:

$$\bar{C}_t = \frac{\bar{T}}{W_{ref}^2 P_{ref}} \quad (5)$$

where, \bar{T} = Mean torsion; \bar{C}_t = Mean torsion coefficient; $W_{ref}^2 = b'd'$ and P_{ref} is as described above.

RESULTS AND DISCUSSIONS

Variation of Mean Pressure Coefficients, \bar{C}_p

The variation of mean pressure coefficients for $\theta = 0^\circ$ at 8 different levels with respect to respective levels, 'z' are shown in Figure 4. For $\theta = 0^\circ$, the mean pressure distribution around the ellipse is observed to be symmetric with respect to major axis, as expected. The positive (+ve) pressure coefficient value is observed over a region i.e., circumferential length of 5.18 cm (2.59 cm on either side with respect to the stagnation ports viz. 1, 29, 57, 85, 113, 141, 169, 197 at Levels 1 to 8, where the value of mean C_p is equal to 1. After a chord length of 2.59 cm on either side with respect to stagnation ports, the negative (-ve) pressure coefficient value is observed to increase over circumferential length up to 8.76 cm, beyond which it is observed to reduce and become relatively minimum -ve pressure, due to pressure recovery in the leeward zone. The values of -ve mean C_p at Level 1 to Level 7 are comparable over the length between 5.256 cm and 14.015 cm. Relatively lesser values of -ve mean C_p are observed at Level 8 over the length specified above, which could be to the presence of free edge, where the flow takes place over roof of the model. The region from 22.776 cm \pm 1.752 cm is observed

to be the base pressure region, where the -ve pressure coefficient values are almost constant. The variation of mean pressure coefficients for $\theta = 90^\circ$ at 8 different levels with respect to 'z' are shown in Figure 5. The mean pressure distribution around the ellipse is observed to be symmetric with respect to minor axis, as expected. The +ve pressure coefficient value is observed to act over a region i.e., circumferential length of 16.9 cm (8.45 cm on either side with respect to stagnation ports viz. 8, 36, 64, 92, 120, 148, 176, 204 at Levels 1 to 8, where the value of mean C_p is equal to 1. After a chord length of 8.45 cm on either side with respect to the stagnation ports, the -ve pressure coefficient value is observed to increase up to the ports which are located perpendicular to the direction of wind and beyond which the -ve pressure coefficient value is observed to remain nearly constant, due to large wake created behind the bluff body. The circumferential lengths over which the +ve or -ve pressure coefficient values are observed, are given in the Table 1 for Level 1 and are found to be dependent on the angle of wind incidence.

Variation of Correlation Coefficients of Fluctuating Pressures

Figure 6(a & b) shows the variation of correlation coefficients between the ports aligned vertically on the windward face at stagnation point for $\theta = 0^\circ$ and 90° and the same are presented in Tables 2 and 3. From these Tables, it is seen that the correlation coefficients are positive in nature, and are observed to decrease with increase in spatial intervals between port pair data sets examined. For the angles of wind incidence considered in the present study, port located at top level correlates about 0.1-0.15 to the port located at bottom level. The pressure correlation is found to be relatively higher for the ports which are located immediate below and/or above levels with respect to the port at a specified level. As expected, pressure correlation is found to be 1 at the same location. Further, selected angles of wind incidence viz. $\theta = 0^\circ$ (wind normal to minor axis) and 90° (wind normal to major axis) were also considered for all the ports which are aligned horizontally (along circumferentially) at Level 1 (L1) with respect to windward port near stagnation and are given in Tables 4 and 5 and shown in Figure 6(c). From Figures 4(b), 5(b) and 6(c), it is seen that the distributions of correlation coefficient values are found to be similar to the corresponding mean pressure coefficient distributions.

Variation of Mean Drag, Lift Force and Torsion Coefficients

The mean drag and lift force coefficients are calculated by resolving the force coefficients with respect to the angle of wind incidence. Figure 7(a) shows the variation of mean C_d with angle of wind incidence at L4 by considering the projected width 'b', as reference width. From the Figure 7(a), it is seen that the values of mean C_d increase with change in angle of wind incidence from 0° to 90° . It can be noted that the component of mean force deduced from Y axis was the main contributor to mean drag force. Figure 7(b) shows the

variation of mean C_l with angle of wind incidence at L4 by considering the projected width d' , as reference width. It is noted that the values of mean C_l increase with change in angle of wind incidence from 0° up to 40° and beyond which they are observed to decrease with change in angle of wind incidence. Figure 7(c) shows the variation of mean C_t with angle of wind incidence corresponding to L4 by considering W_{ref}^2 equal to $b'd'$. From Figure 7(c), it is noted the values of mean C_t is observed to increase with change in angle of wind incidence from 0° up to 15° and beyond which it is observed to decrease with change in angle of wind incidence. The values of mean C_t for both 0° and 90° are found to be 0, as expected, due to symmetry about major and minor axes, respectively.

COMPARISON BETWEEN PRESENT STUDY AND LITERATURE

Variation of Mean Pressure Coefficients

Comparison on variation of mean C_p between the present study ($b/d = 0.5$) on 3D elliptical cylinder at L4 and the literature (Wiland, 1968) on 2D elliptical cylinder ($b/d = 0.6$, under uniform flow) were made and are shown in Figure 8 for $\theta = 0^\circ$ and 90° , respectively. Figure 8(a) shows the comparison on variation of mean C_p for $\theta = 0^\circ$. The values of mean C_p are comparable for normalised circumferential length between 0.03 and 0.22 and between 0.85 and 1. The difference in magnitudes in mean C_p for the circumferential length between 0.22 and 0.85 is attributed to 2D and 3D wind flow with terrain effect. Figure 8(b) shows the comparison on variation of mean C_p for $\theta = 90^\circ$. Both the distributions are comparable upto normalised circumferential length of 0.5 and beyond which the evaluated values are found to be lower when compared with the values reported in the literature.

Variation of Mean Drag and Lift Force Coefficients

Comparison on variation of mean C_d and C_l between the present study and the literature (Cook(1985) on long elliptical cylinder and Wiland (1968) on 2D elliptical cylinders) were made and are shown in Figure 9. It is to be noted that the variation of mean drag force coefficients was obtained by substituting the evaluated values of mean C_d for $\theta = 0^\circ$ and 90° in the empirical equation given in Cook (1985). From Figure 9(a), in general, it is observed that the values of mean C_d are minimum at 0° and maximum at 90° i.e., values of mean C_d increase with change in angle of wind incidence from 0° to 90° . The value of mean C_d reported by Wiland (1968) for 0° is 0.43 which is found to be relatively higher than the evaluated value and the value obtained using empirical equation given in Cook (1985). For $\theta = 90^\circ$, the evaluated value and the value obtained using empirical equation given in Cook (1985) are found to be relatively lower than those reported by Wiland (1968).

Comparison on variation of mean C_l is shown in Figure 9(b). It is to be noted that the variation of mean lift force coefficients was obtained by substituting the evaluated value

of mean C_l for $\theta = 45^\circ$ in the empirical equation given in Cook (1985). From Figure 9(b), it is observed that the values of mean C_l reported in the literature (Cook, 1985 and Wiland, 1968) and the evaluated value are found to be 0 for 0° and 90° . The values of mean C_l increase with change in angle of wind incidence up to certain angle of wind incidence and beyond which it decrease with change in angle of wind incidence. The maximum values of mean C_l reported by Cook (1985) and Wiland (1968) are found to be 0.47 (for $\theta = 45^\circ$) and 0.41 (for $\theta = 50^\circ$), whereas, from the present study it is observed to be 0.49 (for $\theta = 40^\circ$).

COMPARISON BETWEEN PRESENT STUDY AND CODES OF PRACTICE

Values of Mean Drag Force Coefficients

Comparison on values of mean C_d between the present and the values reported in Codes of Practice (IS: 875 and AS-NZS) were made and are shown in Figure 10 for $\theta = 0^\circ$ and 90° , respectively. From Figure 10(b) for $\theta = 0^\circ$, it is found to that the evaluated value of mean C_d is comparable with the values reported in Codes of Practice (IS: 875 and AS-NZS) i.e., for the case of $V_{zb} \geq 10$ m/s and AS/NZS: bVdes, $0 > 10$ m/s. From Figures 10(a & b) for $\theta = 90^\circ$, the % difference between the evaluated value of mean C_d and the value reported in IS: 875 is found to be within 10 %, whereas, the evaluated value are observed to be lesser than the values reported in AS-NZS, could be due to 2D flow on infinite length of cylinder. It is to be noted that the values of force coefficients reported in IS: 875 are for clad buildings of uniform section (plan shape: ellipse) under uniform flow on finite length of cylinder.

CONCLUDING REMARKS

Based on the pressure measurement study, the following conclusions were drawn:

The mean pressure distribution around the ellipse are observed to be symmetric about major and minor axes for $\theta = 0^\circ$ and 90° , as expected. The values of mean pressure coefficients are found to be unity at the stagnation ports of all levels. In the leeward region, the magnitude of -ve pressure coefficients are relatively lower for $\theta = 0^\circ$ when compared with the magnitudes for $\theta = 90^\circ$, due to large wake created behind the model. Hence, the scatter in mean pressure coefficients is insignificant at the windward region, whereas, more scatter is observed in leeward region along the height of the model.

The +ve pressures acting over a length in circumferential direction are observed to increase with change in angle of wind incidence between 0° and 90° , due to the exposure of surface length with respect to flow direction.

The component of mean force deduced from Y axis was mainly contributing to mean drag force. The values of mean C_d is observed to increase with change in angle of wind incidence from 0° to 90° . The values of mean C_l increased with change in angle of wind incidence from 0° up to 40° and beyond which they decrease with change in angle of wind incidence. The values of mean C_t increase with change

in angle of wind incidence from 0° up to 15° and beyond which they decrease with change in angle of wind incidence. The pressure correlations are found to be +ve and/or -ve (due to location dependent with respect to flow direction), and the coefficients decreased with increase in spatial intervals between port pair data sets examined either vertically and/or horizontally. As expected, pressure correlation is found to be unity at the same location. The distributions of correlation coefficient values are found to be similar to the corresponding mean pressure coefficient distributions.

The evaluated values of mean pressure coefficients are found to lower than the values reported in the literature in the leeward region for the angles of wind incidence examined. The evaluated values of mean drag force coefficients for $\theta = 0^\circ$ and 90° are found to be lower than the values reported in the literature.

For $\theta = 0^\circ$, the evaluated value of mean C_d is comparable with the values reported in Codes of Practice (IS: 875 and AS/NZS) i.e., for the case of $V_{zb} \geq 10$ m/s and AS/NZS: bVdes, $0 > 10$ m/s. For $\theta = 90^\circ$, the % difference between the evaluated value of mean C_d and the value reported in IS: 875 is found to be within 10 %, whereas, the evaluated value are observed to be lesser than the values reported in AS-NZS, could be due to 2D flow on infinite length of cylinder.

Future Scope of Work

The effect of plan ratio (b/d) and aspect ratio (h/b) over a range, flow condition (uniform or boundary layer flow) on force coefficients of 3D bluff bodies with elliptic cross-section can be considered for further studies either experimentally (wind tunnel) or numerically (Computational Fluid Dynamics).

ACKNOWLEDGEMENTS

This paper is being published with kind permission of Director, CSIR-SERC, Chennai. Authors thank all the Staff of WEL for their help and co-operation in successful conduct of wind tunnel experiment including model fabrication and instrumentation.

NOTATIONS AND SYMBOLS

b	Minor axis of the elliptic model
b'	Projected width, perpendicular to the direction of wind
CC _{ij}	Correlation coefficient of fluctuating pressures
\bar{C}_d, \bar{C}_l	Mean drag, lift force coefficients, respectively
\bar{C}_p	Mean pressure coefficient
$C_{p,i}(t)$	Instantaneous pressure coefficients at the ith Level in time 't'
$\bar{C}_{p,i}(t)$	Mean pressure coefficients at the ith Level in time 't'
\bar{C}_t	Mean torsion coefficient
d	Major axis of the elliptic model
d'	Projected width, in the direction of wind
F_x, F_y	Forces along body fixed X and Y axes, respectively
\bar{F}_d, \bar{F}_l	Mean drag, lift forces in the direction, perpendicular to the direction of wind,

h	Height of the elliptic model
$p_i(t)$	Instantaneous pressures at the ith Level in time 't'
p_{ref}	Reference pressure
T	Averaging period
\bar{T}	Mean torsion
\bar{U}_{ref}	Mean wind velocity at reference height
W_{ref}	Reference width
z	Instrumentation level
θ	Angle of wind incidence
	Power law coefficient
ρ	Mass density of air
σ_{ij}	Covariance of wind pressures between ports i and j
σ_I, σ_j	Standard deviation of wind pressures at ports i and j

REFERENCES

- [1] Alonso, G., Meseguer, J., Sanz-Andrés, A. and Valero, E., "On the galloping instability of two-dimensional bodies having elliptical cross-sections", oa.upm.es/9597/2/INVE-MEM_2010_88067.pdf.
- [2] AS/NZS 1170.2:2011, "Structural Design Actions, Part 2 – Wind actions"
- [3] Cook, N.J., "Designers guide to wind loading of building structures", Part 2 Static structures, Building Research Establishment, 1985.
- [4] Dikshit, A.K., "On the Unsteady Aerodynamics of Stationary Elliptic Cylinder during Organized Wake Condition", M.A.Sc., Dissertation, 1970.
- [5] Fábio Basaglia Fonseca, Sérgio Said Mansur and Edson Del Rio Vieira, "Flow around elliptical cylinders in Moderate Reynolds Numbers", Proc. of the 22nd International Congress of Mechanical Engineering (COBEM 2013), November 3-7, Ribeirão Preto, SP, Brazil, pp. 4089-4100, 2013.
- [6] IS: 875 (part 3)-1987, "Code of practice for design loads (other than Earthquake) for Buildings and structures- Part 3: Wind loads", BIS, New Delhi.
- [7] Ryan Merrick and Girma Bitsuamlak, "Shape effects on the wind-induced response of High-rise buildings", Journal of Wind and Engineering, Vol. 6, pp. 1-18, 2009.
- [8] Simiu, E. and Scanlan, R.H., "Wind Effects on Structures", 2nd Edition, John Wiley and sons, 1996.
- [9] Takashi Takeuchi, Junji Maeda, Tomohiko Hayata and Hiromasa Kawashita, "Effects of section size on aerodynamic forces on an elliptic cylinder under short-rise-time gusts", Proc. of the Seventh Asia-Pacific Conference on Wind Engineering (website: www.iawe.org), November 8-12, Taipei, Taiwan, 2009.
- [10] Wiland, E., "Unsteady aerodynamics of stationary elliptic cylinder in subcritical flow", M.A.Sc., Dissertation, 1968.

Table 1. Circumferential length over +ve / -ve pressure acts around the elliptical cylinder at Level 1 for different angles of wind incidence

Angle of wind incidence (θ)	+ve pressure over circumferential length	-ve pressure over remaining length
0°	5.18	43.66
10°	5.40	43.44
15°	6.89	41.95
20°	6.88	41.96
30°	10.37	38.47
40°	12.12	36.72
45°	10.36	38.48
50°	12.09	36.75
60°	13.72	35.12
70°	13.83	35.01
75°	13.83	35.01
80°	13.83	35.01
90°	16.90	31.94

Table 2. Correlation coefficients between the ports aligned vertically for $\theta = 0^\circ$

Ports	1	29	57	85	113	141	169	197
1	1.00	0.71	0.52	0.32	0.19	0.17	0.14	0.13
29	0.71	1.00	0.78	0.47	0.31	0.26	0.21	0.19
57	0.52	0.78	1.00	0.60	0.39	0.32	0.23	0.20
85	0.32	0.47	0.60	1.00	0.62	0.51	0.40	0.37
113	0.19	0.31	0.39	0.62	1.00	0.82	0.66	0.59
141	0.17	0.26	0.32	0.51	0.82	1.00	0.82	0.74
169	0.14	0.21	0.23	0.40	0.66	0.82	1.00	0.92
197	0.13	0.19	0.20	0.37	0.59	0.74	0.92	1.00

Table 3. Correlation coefficients between the ports aligned vertically for $\theta = 90^\circ$

Ports	8	36	64	92	120	148	176	204
8	1.00	0.76	0.61	0.42	0.29	0.25	0.19	0.15
36	0.76	1.00	0.82	0.55	0.39	0.34	0.28	0.23
64	0.61	0.82	1.00	0.70	0.51	0.43	0.34	0.28
92	0.42	0.55	0.70	1.00	0.73	0.60	0.46	0.39
120	0.29	0.39	0.51	0.73	1.00	0.90	0.75	0.65
148	0.25	0.34	0.43	0.60	0.90	1.00	0.88	0.78
176	0.19	0.28	0.34	0.46	0.75	0.88	1.00	0.95
204	0.15	0.23	0.28	0.39	0.65	0.78	0.95	1.00

Table 4. Correlation coefficients between the ports aligned horizontally for $\theta = 0^\circ$ at L1

port 1-1	port 1-2	port 1-3	port 1-4	port 1-5	port 1-6	port 1-7	Port 1-8	port 1-9
1.00	0.41	-0.09	-0.34	-0.56	-0.57	-0.60	-0.62	-0.57
port 1-10	port 1-11	port 1-12	port 1-13	port 1-14	port 1-15	port 1-16	Port 1-17	port 1-18
-0.47	-0.33	-0.16	-0.05	-0.04	-0.02	0.03	0.02	-0.04
port 1-19	port 1-20	port 1-21	port 1-22	port 1-23	port 1-24	port 1-25	Port 1-26	Port 1-27
-0.18	-0.45	-0.62	-0.68	-0.68	-0.66	-0.60	-0.62	-0.38
port 1-28								
-0.01								

Table 5. Correlation coefficients between the ports aligned horizontally for $\theta = 90^\circ$ at L1

port 8-1	Port 8-2	port 8-3	port 8-4	port 8-5	port 8-6	port 8-7	Port 8-8	port 8-9
-0.19	-0.25	-0.40	0.01	0.45	0.76	0.95	1.00	0.93
port 8-10	Port 8-11	port 8-12	port 8-13	port 8-14	port 8-15	port 8-16	Port 8-17	port 8-18
0.79	0.60	0.18	-0.22	-0.23	-0.09	-0.12	-0.15	-0.16
port 8-19	Port 8-20	port 8-21	port 8-22	port 8-23	port 8-24	port 8-25	Port 8-26	port 8-27
-0.17	-0.15	-0.16	-0.17	-0.20	-0.21	-0.22	-0.22	-0.21
port 8-28								
-0.18								

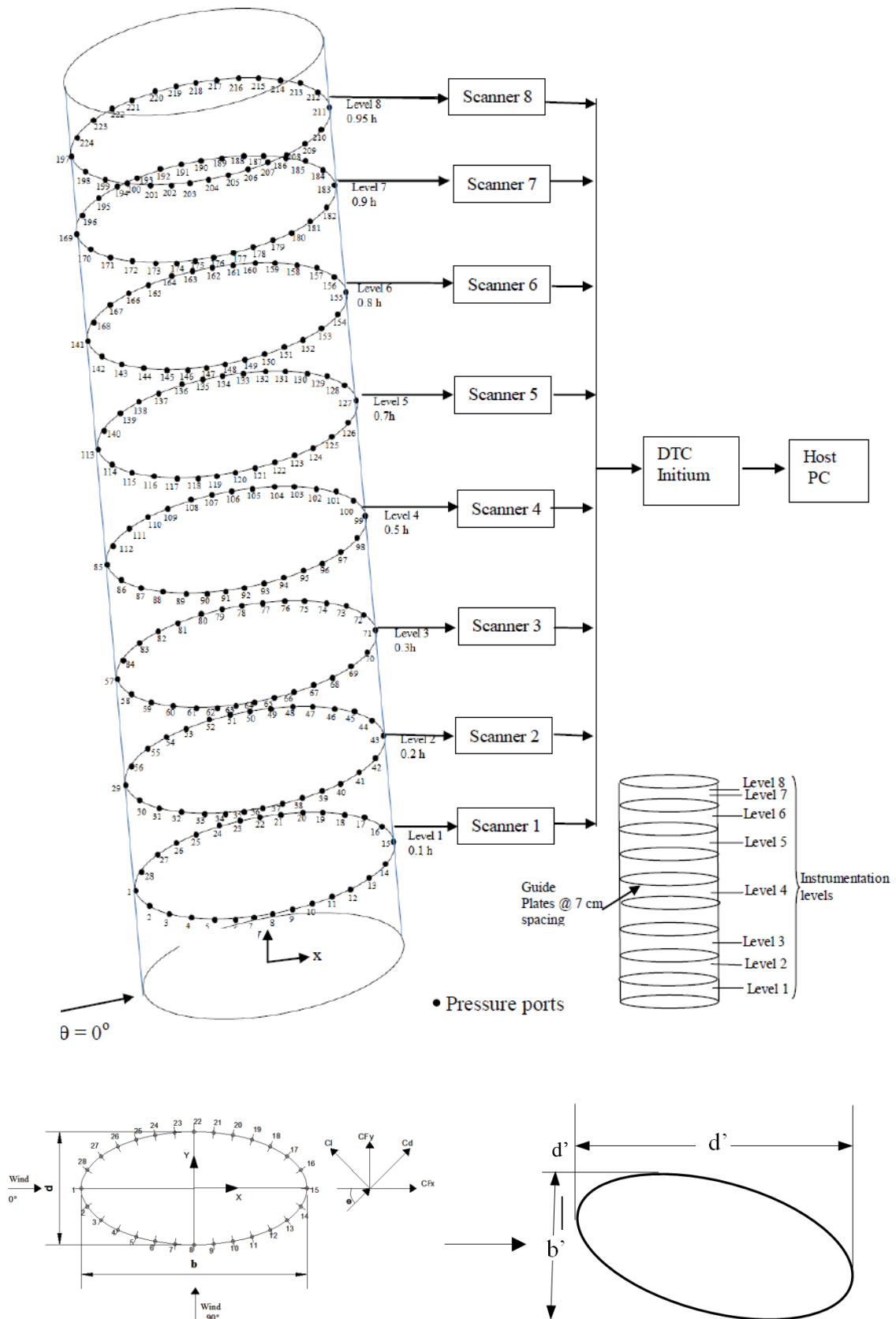


Figure 1. Schematic diagram of pressure measurement system with details pressure ports and orientation of axes

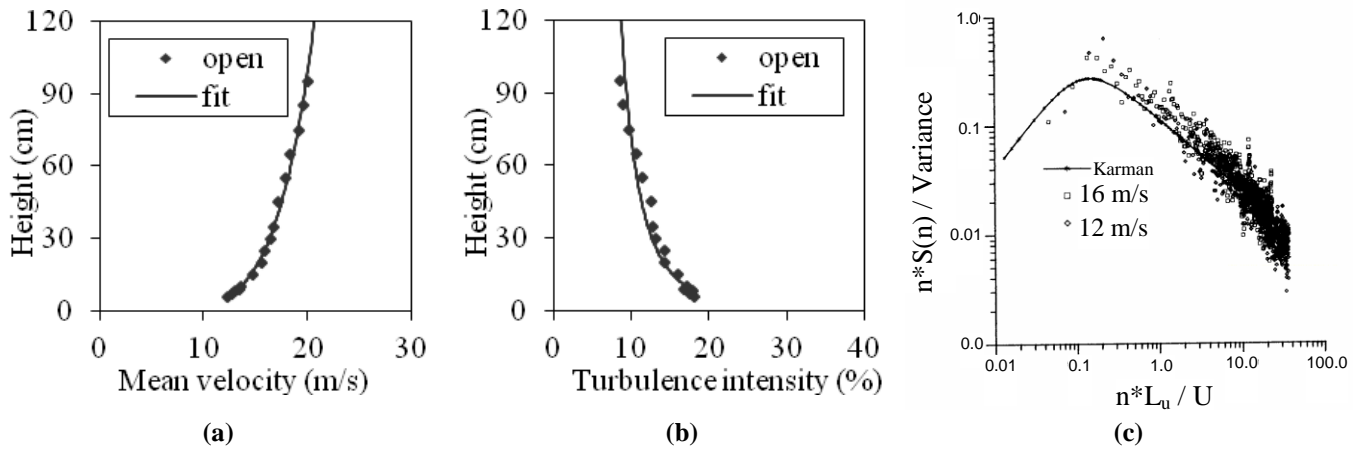
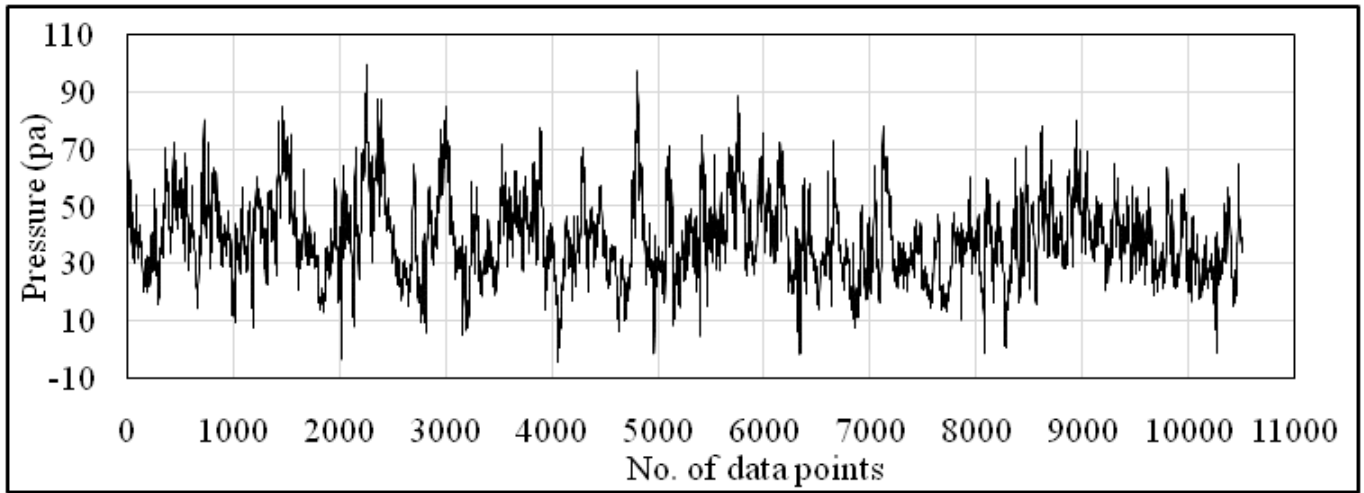


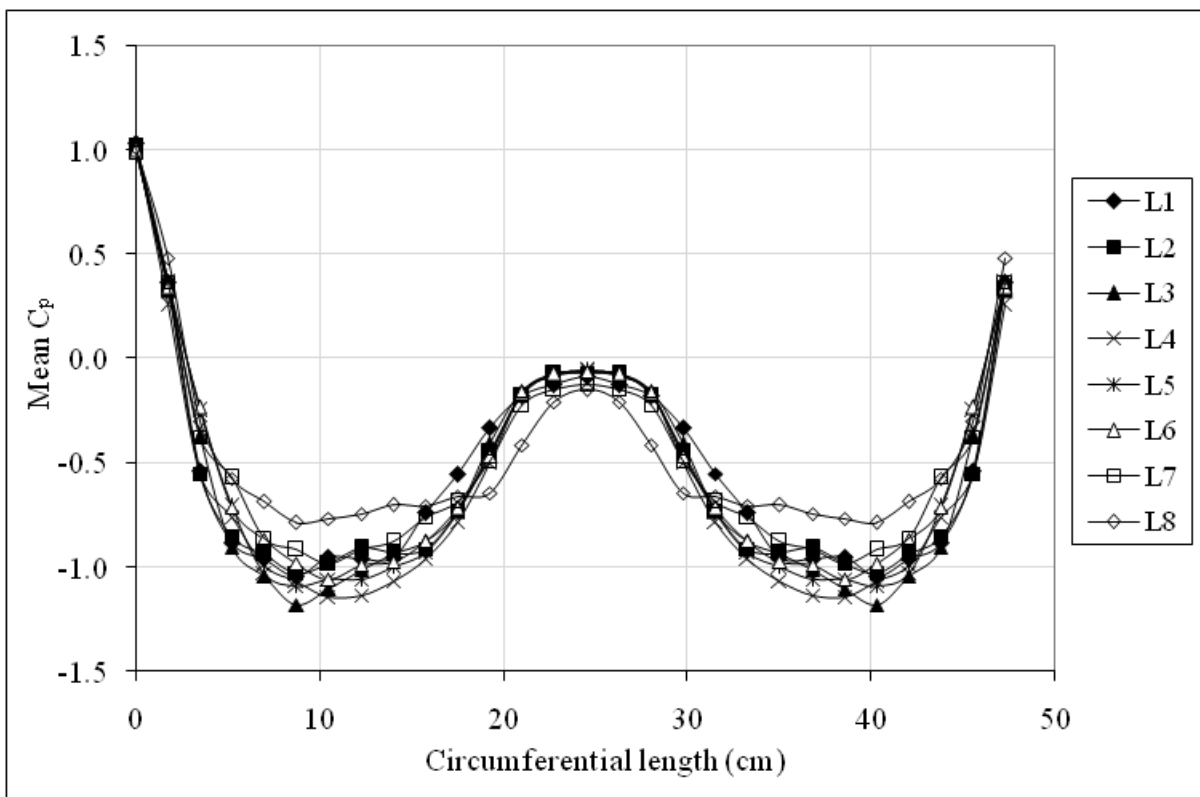
Fig. 2 Simulated wind characteristics in BLWT (a) Mean velocity along height (b) Turbulence intensity along height and (c) Turbulence spectrum of fluctuating wind



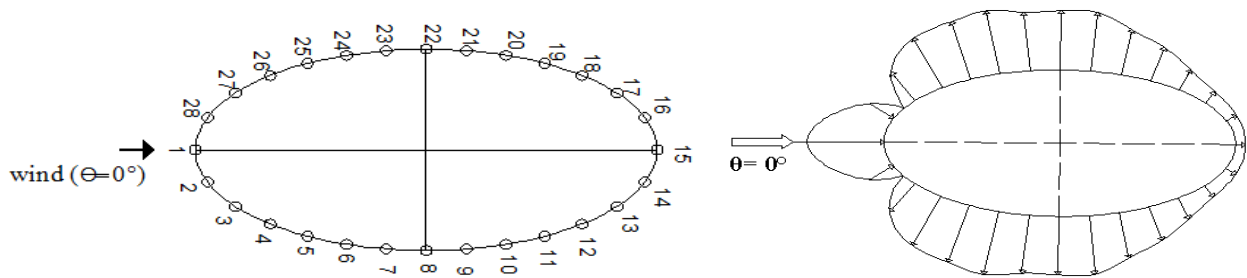
Figure 3. Typical view of tall building model with elliptic cross-section for $\theta = 0^\circ$



(a)

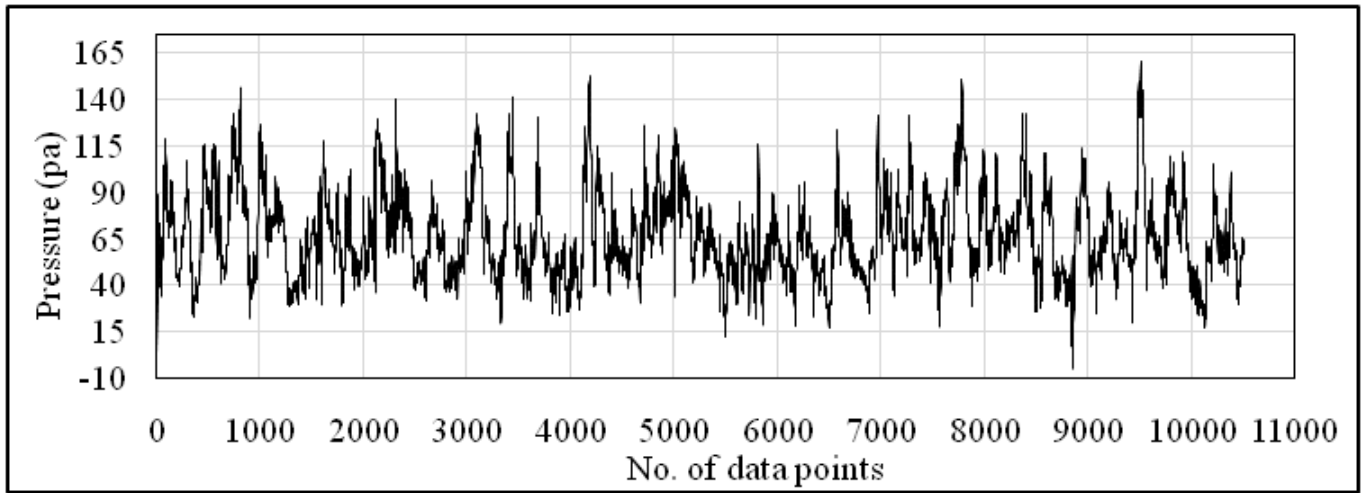


(b)

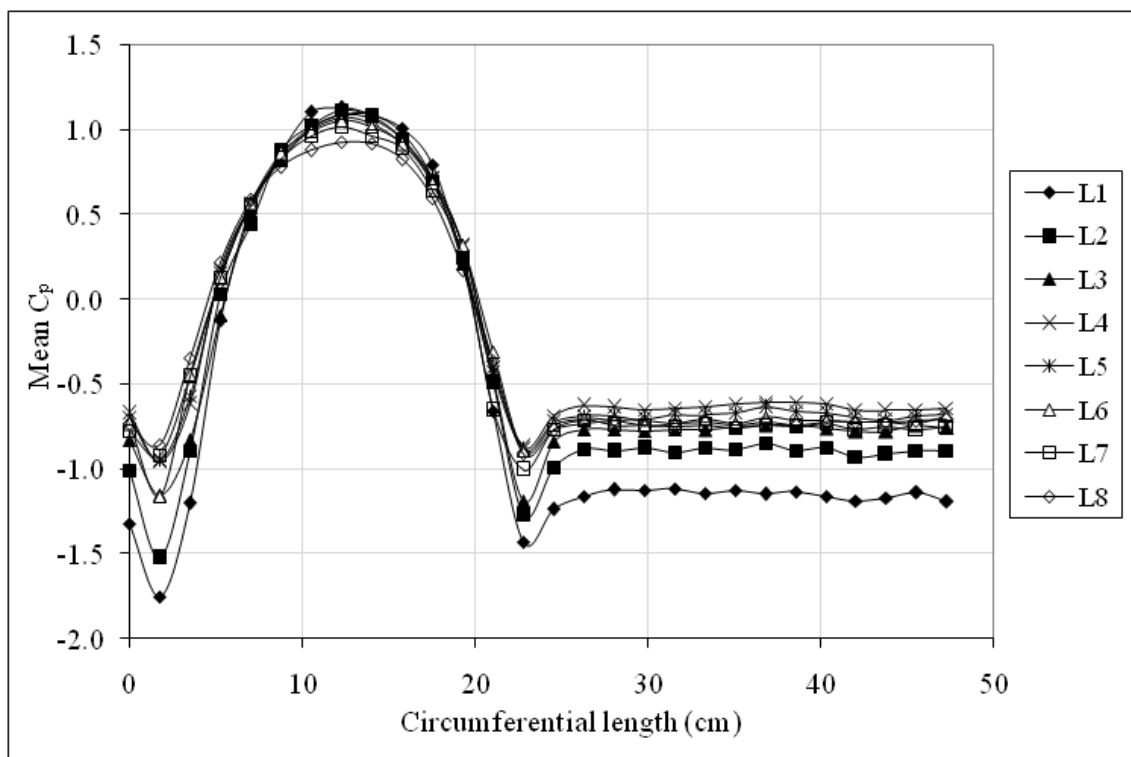


(c)

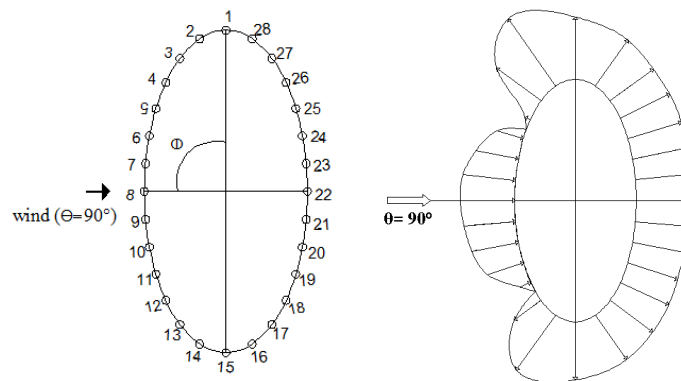
Figure 4.Details on pressure distribution for $\theta = 0^\circ$. (a) Pressure trace at port no. 1, (b) Variation of mean C_p at all levels, (c) Variation of mean C_p around elliptic at Level 1



(a)

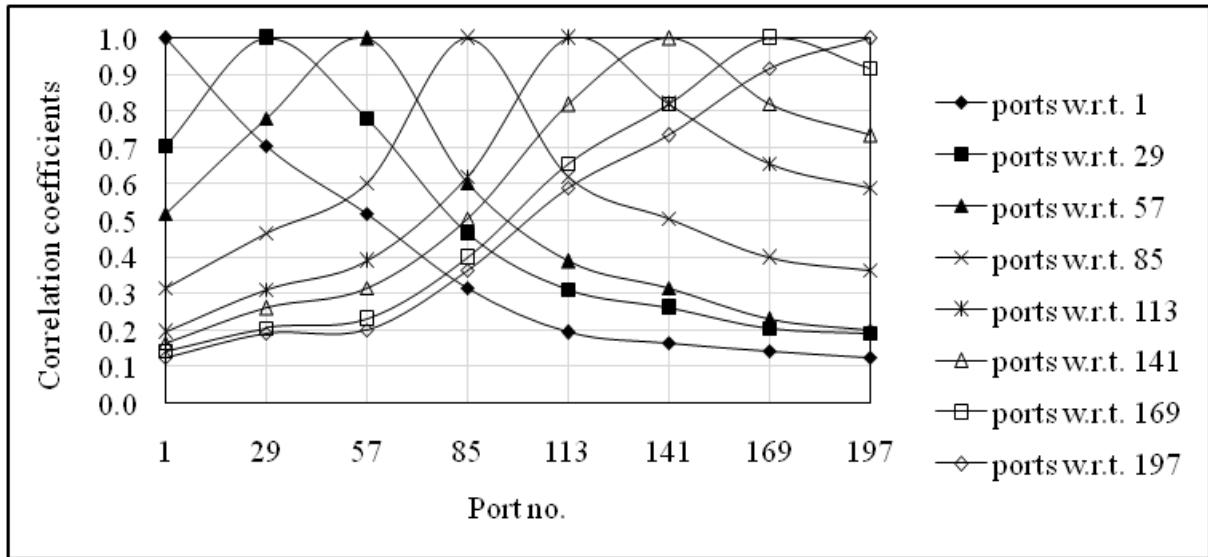


(b)

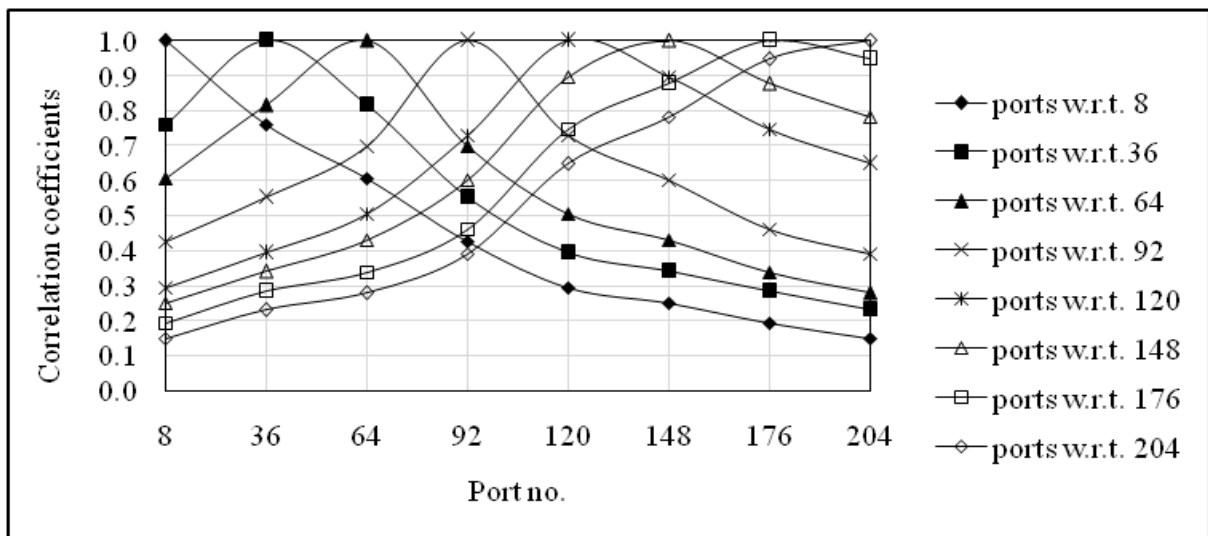


(c)

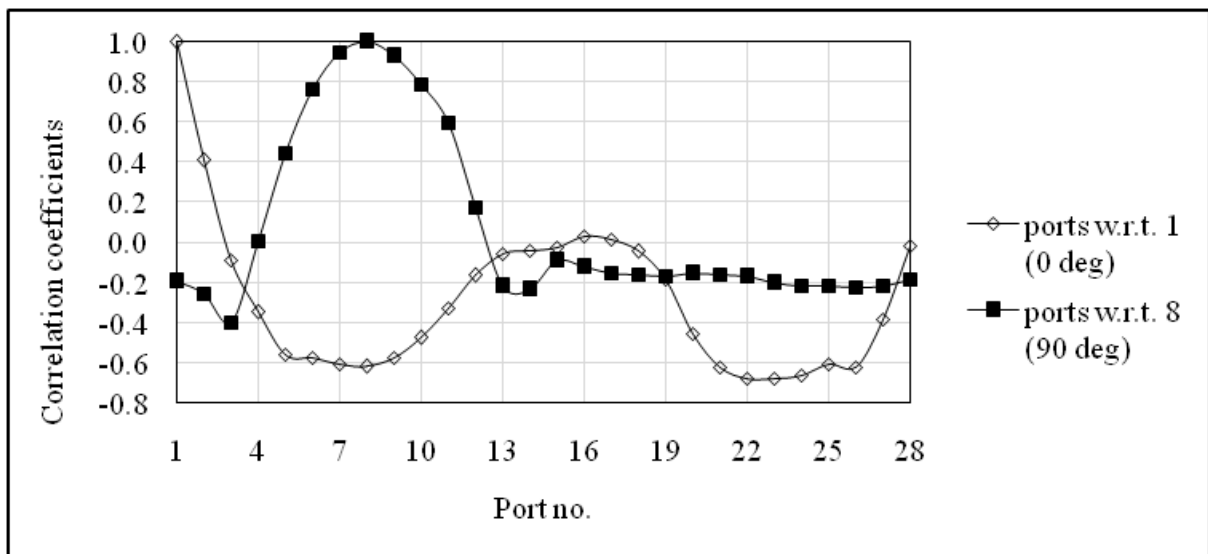
Figure 5. Details on pressure distribution for $\theta = 90^\circ$. (a) Pressure trace at port no. 8, (b) Variation of mean C_p at all levels, (c) Variation of mean C_p around elliptic at Level 1



(a)

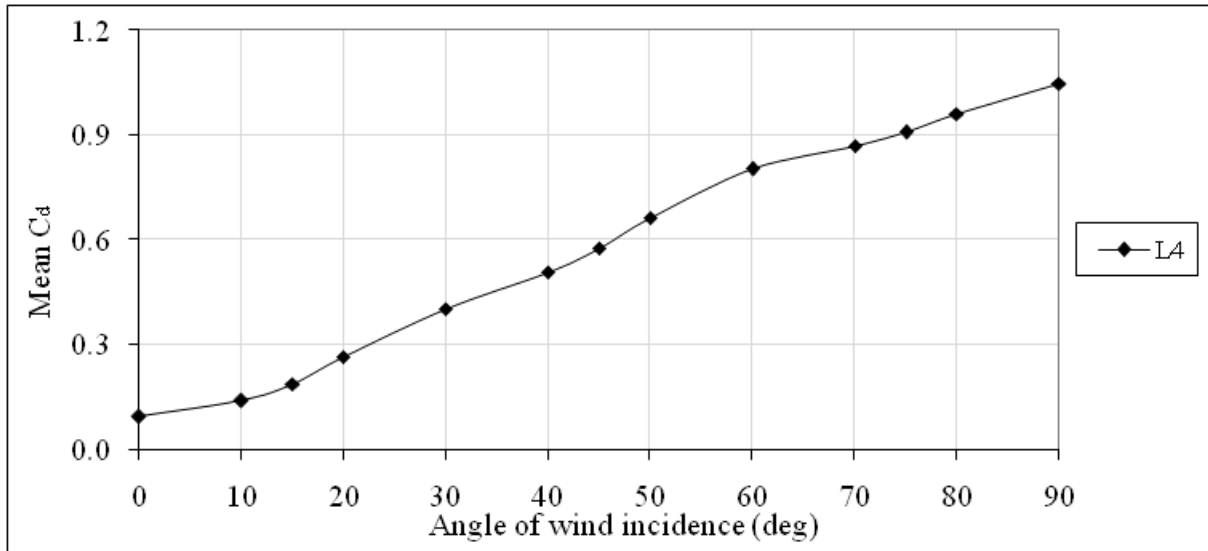


(b)

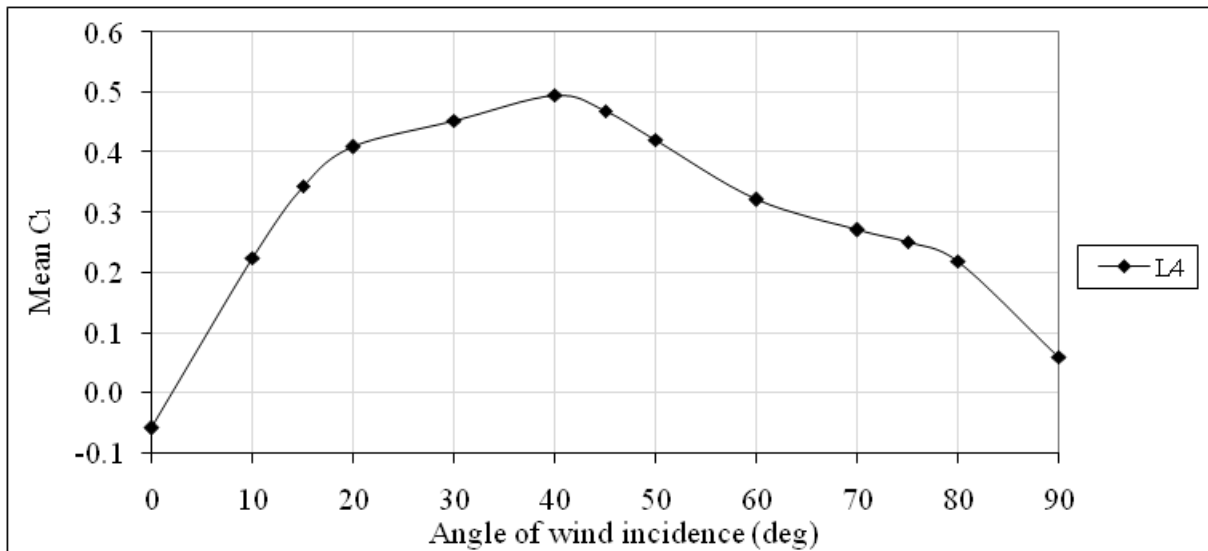


(c)

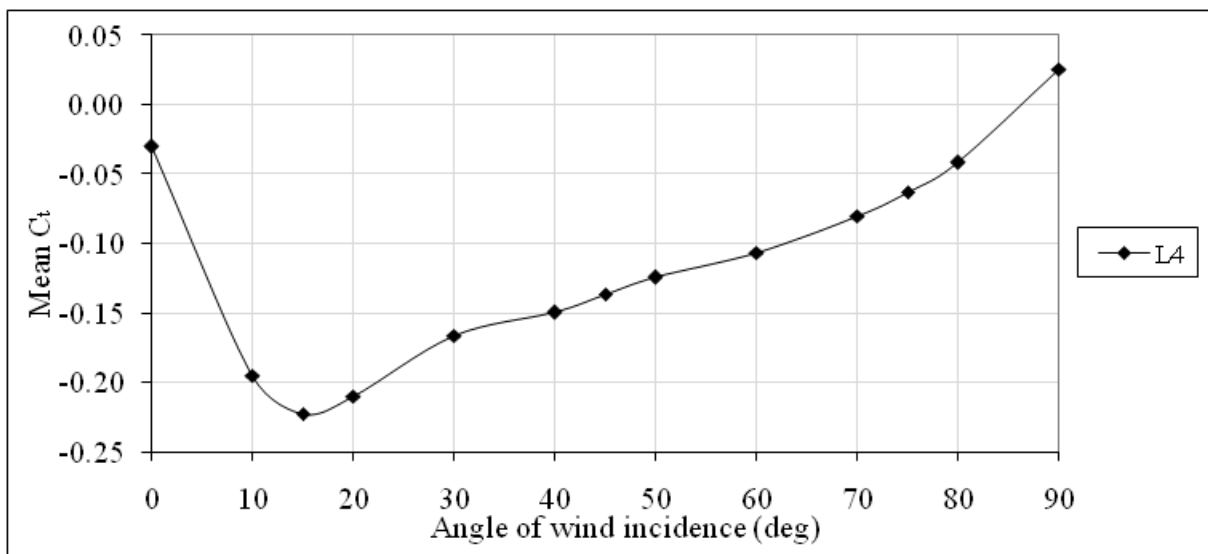
Figure 6. Variation of correlation coefficients. Vertical:(a)0°, (b) 90°and Horizontal:(c) L1



(a)

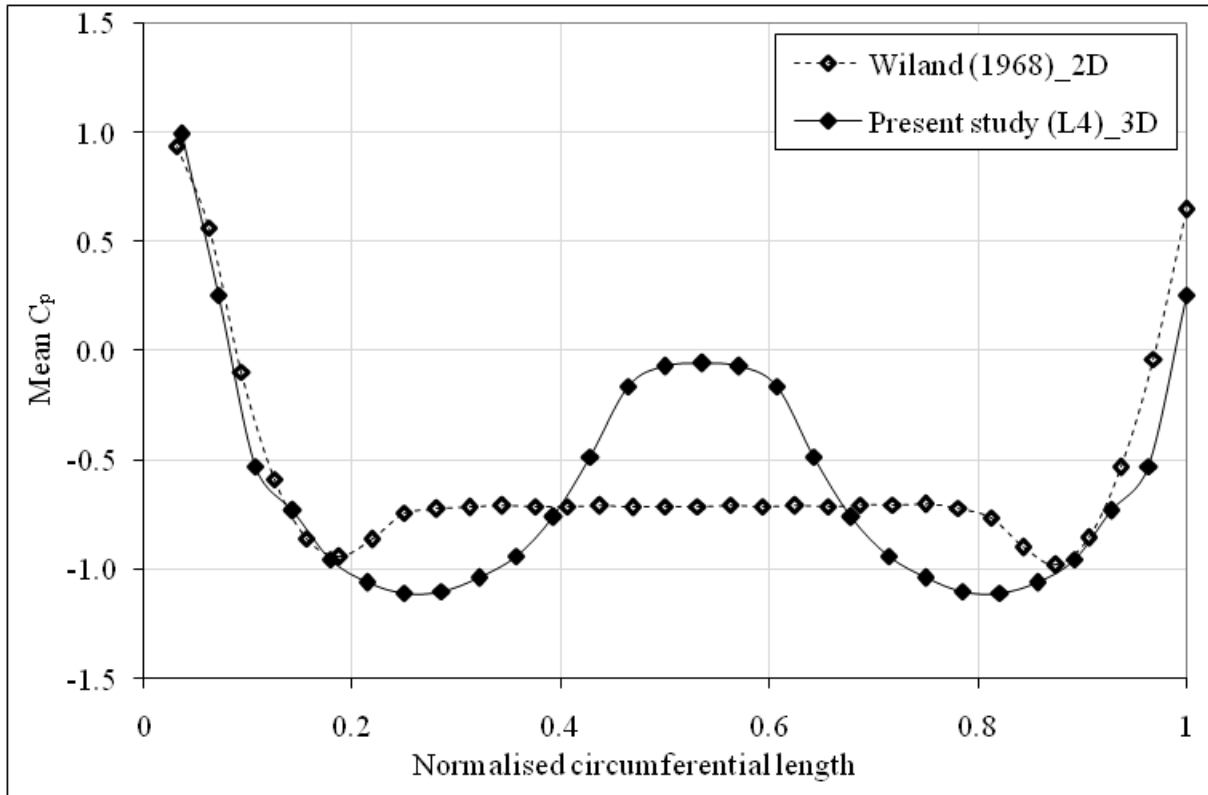


(b)

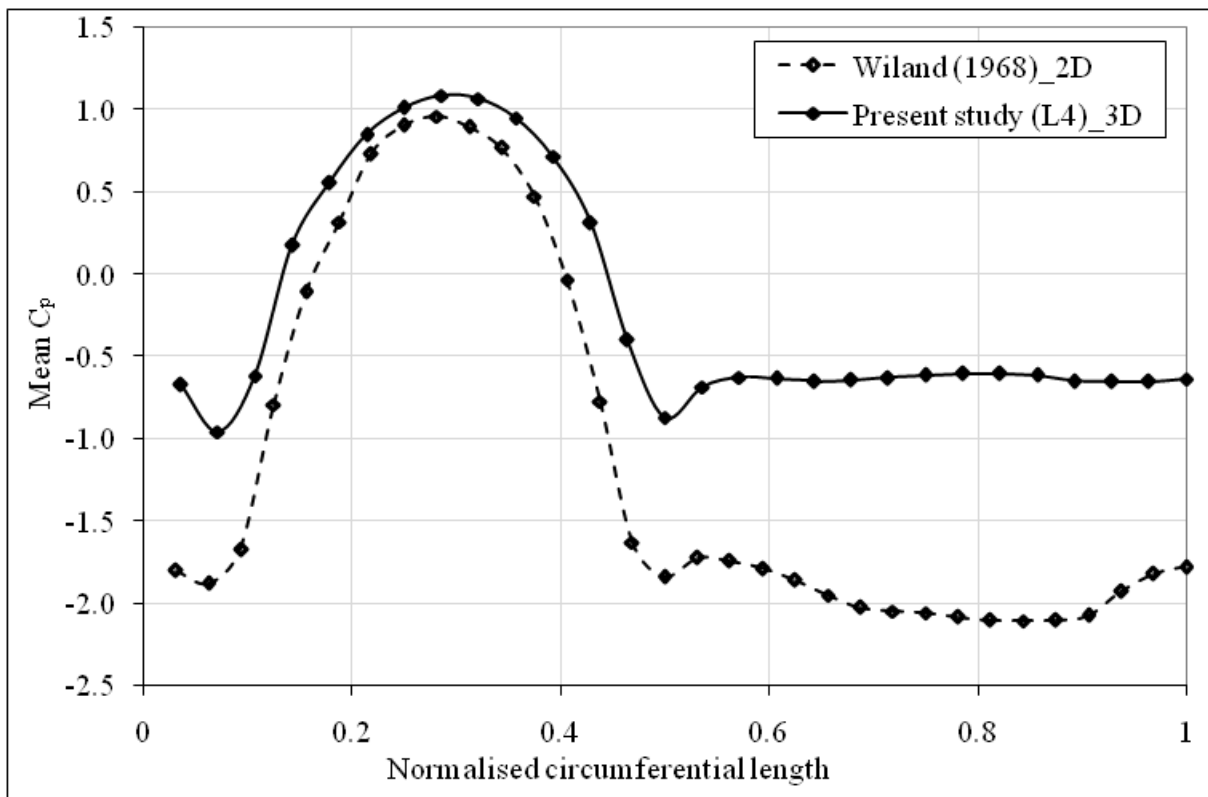


(c)

Figure 7. Variation of mean force/torsion coefficients.(a) Drag, (b) Lift and (c) Torsion

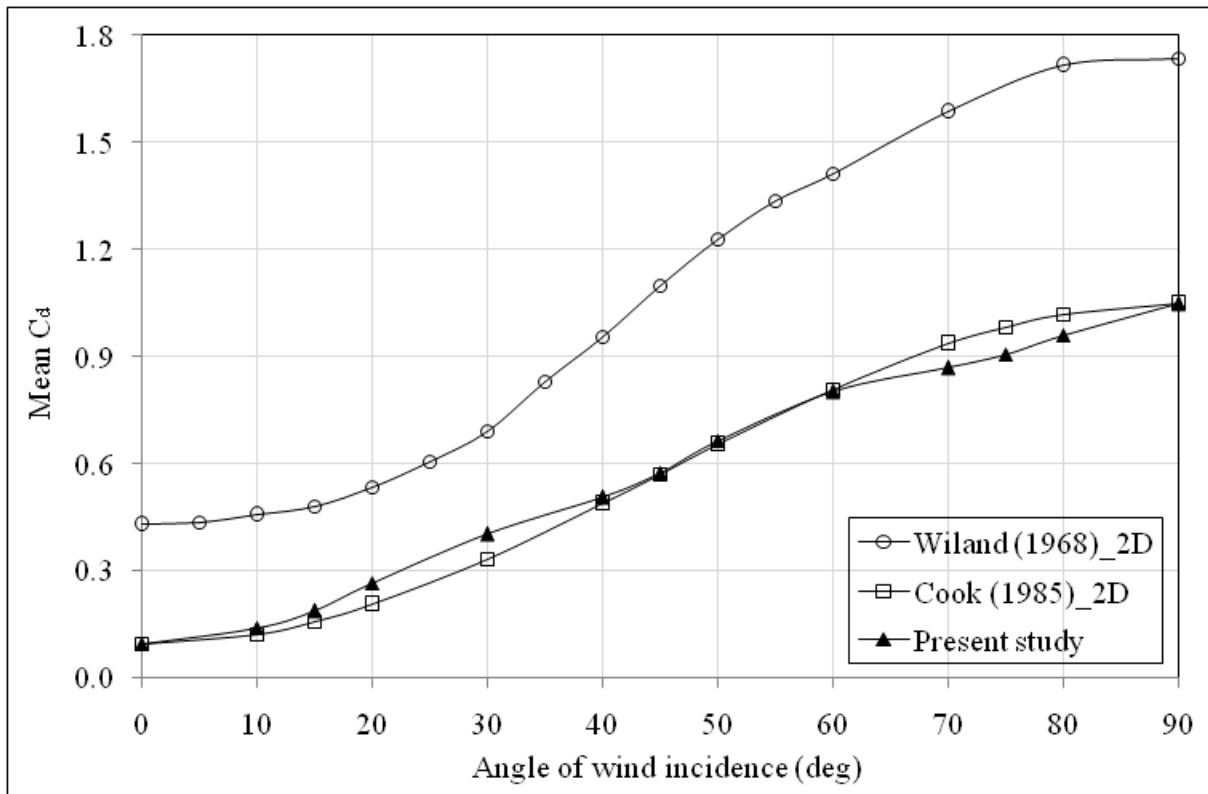


(a)

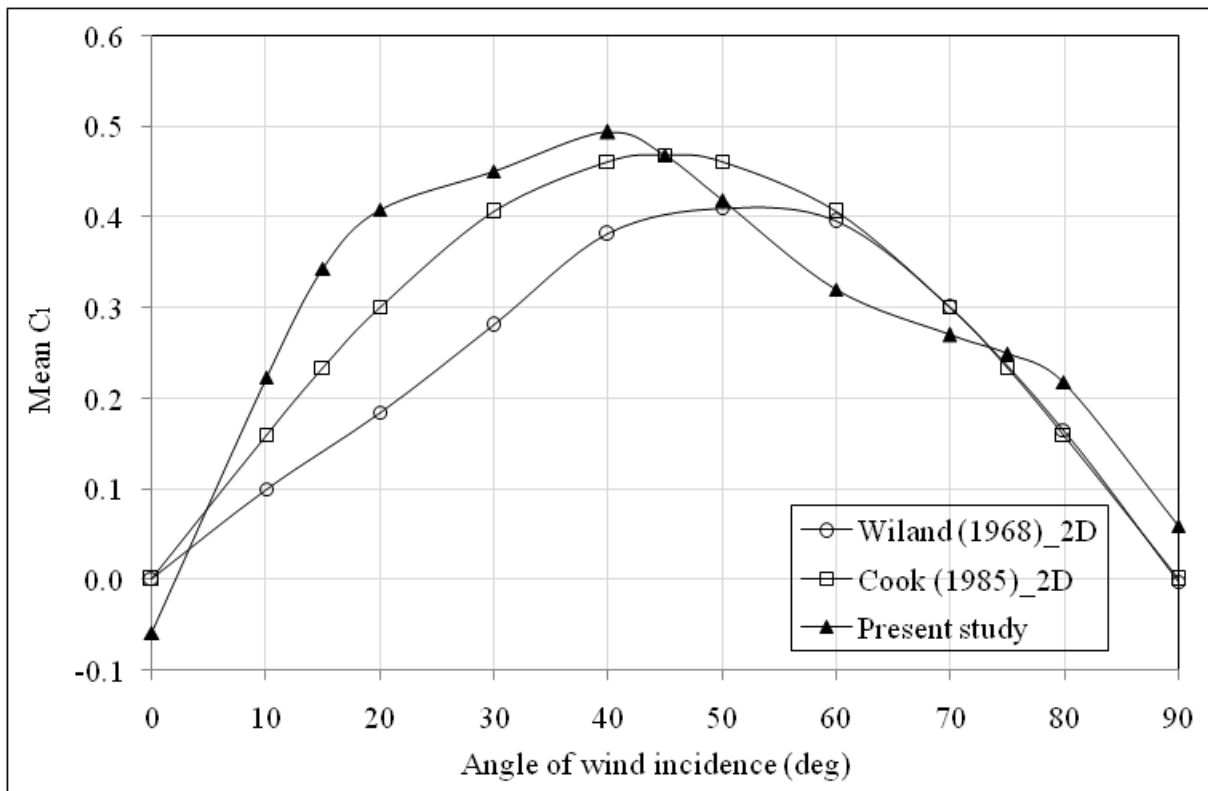


(b)

Figure 8. Comparison of variations on mean pressure coefficintes (a) 0° and (b) 90°



(a)



(b)

Figure 9. Comparison on variation of mean force coefficients. (a) Drag and (b) Lift

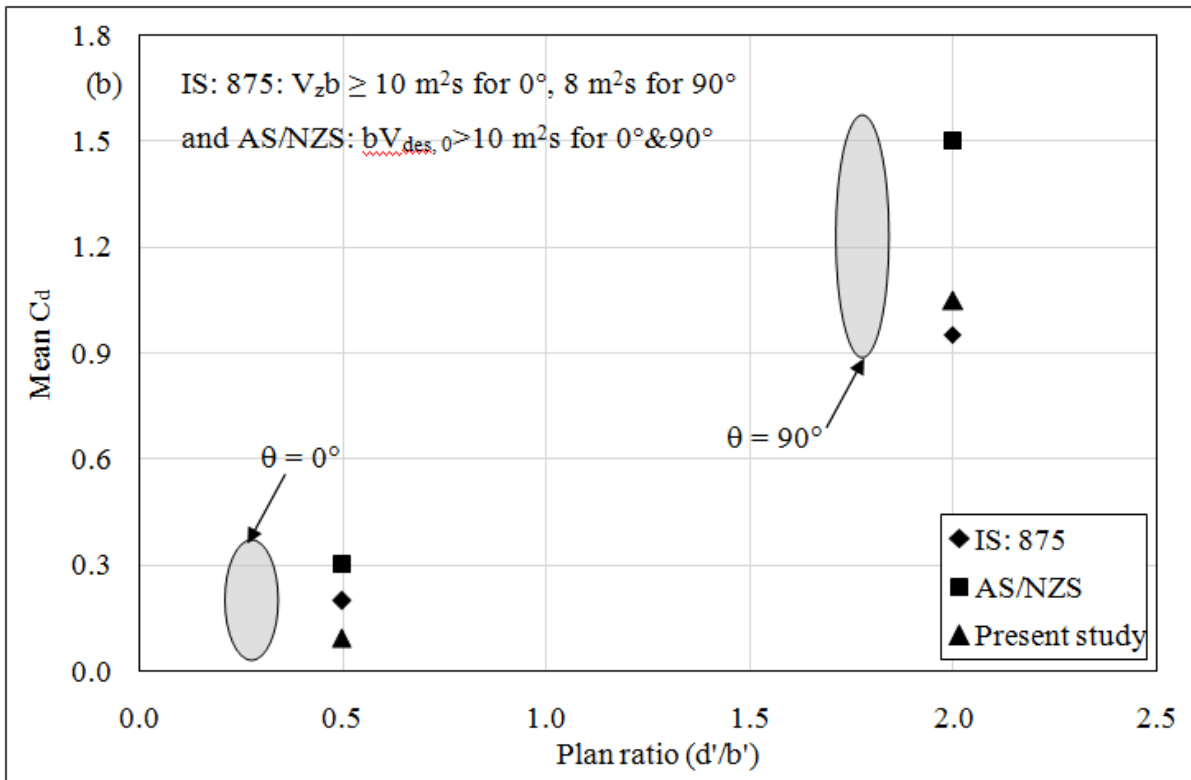
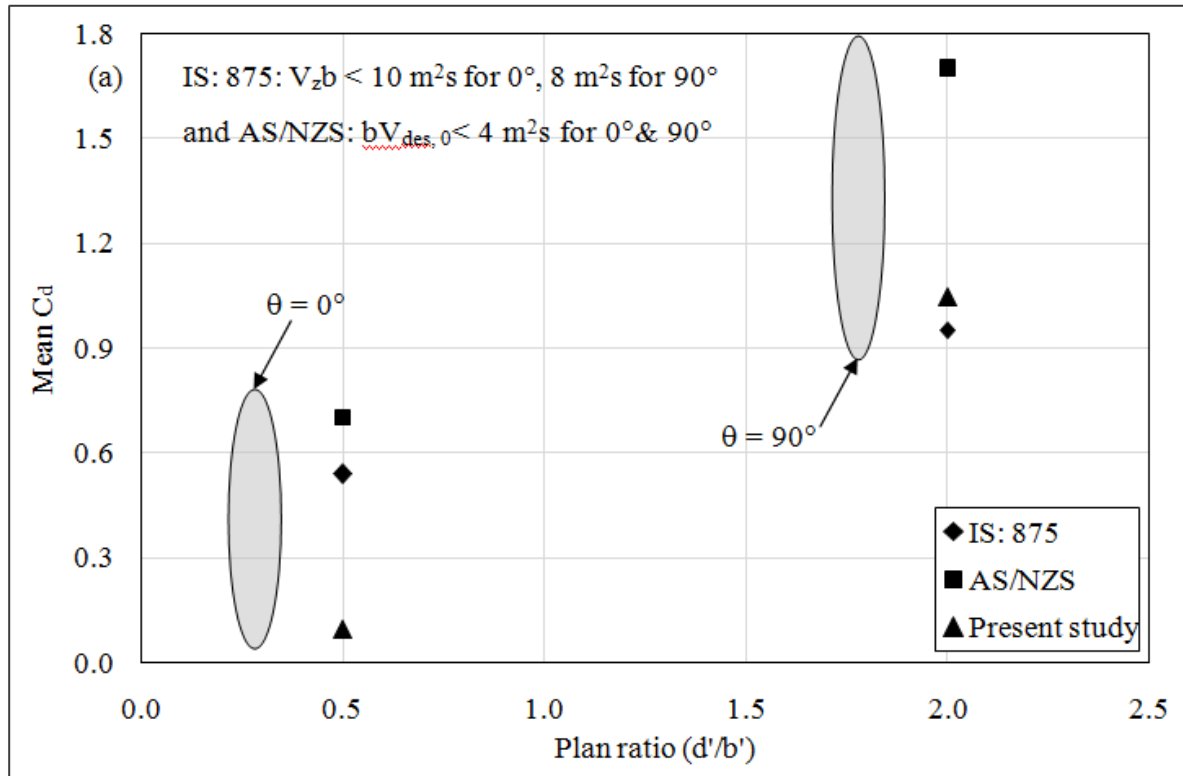


Figure 10. Comparison on drag coefficients between evaluated values and codes of practice